Full Paper

Journal of the Brazilian Chemical Society

https://dx.doi.org/10.21577/0103-5053.20260040

J. Braz. Chem. Soc. **2026**, *37-Spe1*, e-20260040, 1-20

Metabolomic Insights on Plant Growth-Promoting Yeast as Bioinput: Biochemical Interactions with Tomato Seedlings

Miria A. Souza,[a,b] Jorge C. Rodrigues Neto,[a] Eder A. Barbosa,[a] Catharine A. Bomfim,[a] Thais D. Mendes,[a] João R. M. de Almeida,[a] Silvia B. Gonçalves,[a] Félix G. de Siqueira[a] and Patrícia V. Abdelnur[*,a,b]

[a]*Embrapa Agroenergia, Empresa Brasileira de Pesquisa Agropecuária, W3 Norte, PqEB, 70770-901 Brasília-DF, Brazil*

[b]*Instituto de Química, Universidade Federal de Goiás, Campus Samambaia, 74690-900 Goiânia-GO, Brazil*

Plant growth-promoting yeasts (PGPYs)-based bioinputs offer a sustainable approach in agriculture, increasing crop productivity and reducing environmental impacts. However, their chemical interactions with plants remain poorly understood. In this paper, metabolites and metabolic pathways were deeply investigated in tomato seedling leaves inoculated with active (L01AT) and inactive (L01IN) *Sporidiobolus* yeast. Yeast was applied near the roots of the tomato seedlings, and agronomic and metabolomic studies were performed after 40 days. A total of 73 metabolites, including primary and secondary, were annotated using mass spectrometry-based metabolomics. Inoculation of the yeast L01AT promotes more intense changes in the biosynthetic pathways of secondary metabolism compounds, such as phenylpropanoid biosynthesis, such as phenylpropanoid biosynthesis, flavone and flavonol biosynthesis, and anthocyanin biosynthesiss. On the other hand, inoculation of the yeast L01IN promotes changes in the primary metabolic pathways, such as lysine biosynthesis and porphyrin metabolism, which are compounds derived from yeast cell degradation after heating. This integrated agronomic, biological, and chemical analysis provides a comprehensive understanding of the metabolic reprogramming induced by Sporidiobolus inoculation in tomato seedlings. These findings contribute to the design of safer and more efficient bioinput strategies and support the discovery of bioactive compounds for advanced formulation development.

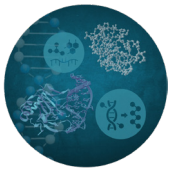

Keywords: mass spectrometry, metabolomics, metabolites, metabolic pathways, sustainable agriculture

Introduction

Agriculture plays a fundamental role in providing food, feed, fiber, and energy. However, the indiscriminate use of agrochemicals has caused soil degradation, groundwater contamination, and ecological imbalances, in addition to favoring pest and disease outbreaks.[1-3] In this scenario, bioinputs emerge as a more sustainable alternative. They stimulate plant development at all stages, provide essential nutrients, increase resistance to biotic and abiotic stresses, and improve soil fertility.[2,4,5] These characteristics can result in higher productivity with less environmental impact and reduced production costs. The adoption of bioinputs has been increasing steadily. In Brazil, a 13% expansion was recorded during the 2024/2025 harvest season, with 156 million hectares treated. Globally, the market is projected to reach approximately US$ 20 billion by 2027, representing nearly a threefold increase compared to its current value.[6]

Biological inputs, or bioinputs, are defined as products, processes, or technologies derived from plant, animal, or microbial sources that positively influence plant growth, development, and response mechanisms.[7]

Microorganisms such as bacteria (e.g., *Rhizobium*, *Azospirillum*, *Bacillus*, *Streptomyces*, *Gluconacetobacter*, and *Pseudomonas*), filamentous fungi (e.g., *Trichoderma*, *Aspergillus*, *Claroideoglomus*, *Glomus*, and *Rhizophagus*) and yeasts (e.g., *Candida* spp., *Rhodotorula* spp., *Cryptococcus* spp., and *Saccharomyces* sp.) have been widely investigated as bioinputs.[8] These organisms have been extensively studied in different plant organs (roots,

*e-mail: patricia.abdelnur@embrapa.br
Editor handled this article: Paulo Wender P. Gomes (Guest)
This publication is part of the special issue "Omics Sciences"

shoots, fruits, and seeds) of crops such as wheat, corn, rice, beans, alfalfa, grapes, pomegranates, beets, and tomatoes.[8]

Among the diverse microorganisms explored as bioinputs, plant growth-promoting yeasts (PGPYs) have gained increasing attention because they enhance plant development under optimal conditions as well as under biotic and abiotic stress. They promote growth through two main mechanisms: direct and indirect.[9] Direct mechanisms include the production of phytohormones such as auxins, cytokinins, and gibberellins, as well as improvements in nutrient bioavailability in the soil, while indirect mechanisms involve biological control of pathogens through antibiotic production, secretion of cell wall-degrading enzymes, and the induction of systemic resistance in plants.[4,9]

Yeasts isolated from vineyards (*Debaryomyces hansenii*, *Lachancea thermotolerans*, and *Saccharomyces cerevisiae*) have been reported[10] to enhance corn seedling development, increasing dry weight and chlorophyll content by approximately 10%. The yeasts *Schwanniomyces etchellsii*, *Zygotorulaspora florentina*, and *Holtermanniella festucosa* were inoculated into zucchini seedlings, promoting increased weight, length, and root development.[11] The yeast *Candida tropicalis* increased root dry weight of rice seedlings by 16-35%, an effect associated with indole-3-acetic acid (IAA) production, 1-aminocyclopropane-1-carboxylate (ACC) deaminase activity, phosphate solubilization, and good root colonization.[12]

Furthermore, the literature[10,11,13] indicates that yeast-based bioinputs, in general, can produce specific compounds, including phytohormones (indole-3-acetic acid, auxins, cytokinins, gibberellins, abscisic acid), stress-related regulators (ethylene, brassinosteroids, jasmonic acid, salicylic acid, and strigolactones), and enzymes (β-1,3-glucanase, exo-β-1,3-glucanase, protease, xylanase, amylase, pectinase, and cellulase). These compounds play key roles in: (*i*) enabling plant adaptation to biotic and abiotic stresses, (*ii*) regulating physiological functions, (*iii*) supporting plant survival and defense against pathogens, and (*iv*) degrading pathogen cell walls.[9,13]

Understanding the chemistry and metabolism of PGPYs and their interaction with host plants is crucial for their effective application in agricultural systems. However, despite their importance, the chemical mechanisms underlying the interactions between PGPYs and plants, particularly those mediated by roots and the plant-associated microbiome, remain poorly understood. This in-depth characterization is important for the development of safer and more sustainable products. Moreover, new molecules with agronomic potential may be discovered, which can be used for a more precise bioinput formulation.

In this context, the use of mass spectrometry-based metabolomics has been increasingly adopted to fill this knowledge gap. Metabolomics is a powerful tool for qualitatively and quantitatively assessing metabolic profiles in biological systems. It enables the identification of key metabolites involved in plant physiology, development, and responses to biotic and abiotic stresses. By characterizing both primary and secondary metabolites, metabolomics provides deeper insight into metabolic networks and pathways in plants and microorganisms. Two main strategies are employed: (*i*) targeted analysis, which focuses on identifying and absolutely quantifying predefined metabolites in specific pathways, and (*ii*) untargeted analysis, or metabolic profiling, which explores a wide range of known and unknown compounds without prior selection.[14-16] This holistic approach supports the understanding of dynamic metabolic changes and the discovery of novel bioactive compounds relevant to agriculture and industry.[14-16]

In this study, the metabolites and metabolic pathways of tomato seedling leaves (*Solanum lycopersicum* cv. BRS Zamir) inoculated with viable *Sporidiobolus* yeast cells (L01AT) and non-viable *Sporidiobolus* yeast cells (L01IN) were analyzed. This yeast was selected as the most effective after an extensive greenhouse study evaluating twenty potential PGPYs strains. To investigate the biochemical mechanisms underlying their effects, mass spectrometry-based metabolomics was employed as a tool for analyzing the metabolic profiles and pathways involved in tomato seedling leaves after PGPYs inoculation. Yeasts of the genus *Sporidiobolus* are known for their ability to produce bioactive compounds that act directly in modulating plant metabolism, favoring plant development and resistance.[17] Such metabolites include exopolysaccharides, lipids, carotenoids, enzymes, and γ-decalactone.[17]

Although studies investigating the role of *Sporidiobolus* spp. in plant growth promotion are still relatively recent and underexplored, evidence points to its effectiveness in both phytohormones production and interactions with the rhizosphere microbiome, making it a promising for agricultural bioinoculants.

Experimental

Materials and reagents

The solvents used were: methanol (liquid chromatography mass spectometry (LC-MS) grade ≥ 99.9%, J.T. Baker), formic acid (LC-MS grade ≥ 99.9%, Merck), acetonitrile (LC-MS grade ≥ 99.9%, Fluka Analytical) and

nitric acid 65% v/v (Sigma-Aldrich). All solutions were prepared with ultrapure water (18.2 MΩ) obtained through the Milli-Q purification system (Millipore).

The yeast strain L01 was obtained from the Collection of Microorganisms and Microalgae Applied to Agroenergy and Biorefineries (CMMAABio) of Embrapa Agroenergia, Brazil. The yeasts were incubated in yeast extract-peptone-dextrose (YPD) liquid medium (containing 1% yeast extract, 2% peptone and 2% dextrose) under constant orbital shaking (180 rpm) at 28 °C for 48 h, with cell growth monitoring through optical density (OD_{600}) measurements in an ultraviolet-visible spectroscopy (UV-Vis). All culture media were previously sterilized by autoclaving (121 °C, 1 atm) for 20 min before inoculation of the microorganisms, thus ensuring aseptic conditions for the execution of the experiments.

Bioassay using yeast

Plant growth promotion mediated by the yeast L01 was evaluated in *Solanum lycopersicum* L. hybrid tomato seedlings BRS Zamir® grown in trays with sterilized commercial soil Maxfertil® in a greenhouse (Figure 1). The substrate used was composed of previously composted and carbonized pine bark, vermiculite, limestone, and a basal NPK (nitrogen-phosphorus-potassium) fertilizer. The material showed a water retention capacity of approximately 90% and a pH close to 6.0. A randomized block design (RBD) with four blocks *per* treatment, consisting of five plants (biological replicates) *per* block, was adopted. Three treatments were evaluated: L01AT, L01IN and the fertilized control (CF).

Treatment L01AT consisted of a suspension containing viable yeast cells at a concentration of 1.11×10^9 CFU (colony forming unit) mL^{-1}. Treatment L01IN consisted of a suspension containing non-viable yeast cells, obtained by autoclaving at 121 °C and 1 atm, and adjusted to the same initial cell concentration (1.11×10^9 CFU mL^{-1}) prior to autoclaving. Seedlings treated with L01AT and L01IN were evaluated using five biological replicates, whereas the control treatment without yeast inoculation (CF) consisted of four biological replicates. The CF treatment comprised four biological replicates due to the failure of one seedling to germinate. Because all treatments were applied at sowing, the missing replicate could not be replaced after emergence. Therefore, to maintain experimental consistency and avoid introducing bias associated with differential treatment timing, the non-germinated replicate was excluded, resulting in four biological replicates for the CF treatment.

After sowing, tomato seedlings (Figure 1) immediately received 1 mL of the yeast suspension as an initial treatment. The yeast was evaluated in the logarithmic microbial growth phase (exponential growth), as previously determined by growth curves monitored by spectrophotometry (λ = 600 nm).

In parallel with yeast inoculation, all experimental units, including L01AT, L01IN, and CF, received 3 mL of a commercial liquid fertilizer NPK 8-8-8 (Polifert®), diluted at a proportion of 10 mL L^{-1}, according to the recommendations of the manufacturer. The yeast treatments were performed in three applications: at the time of sowing (D0), and at 15 (D15) and 30 days (D30) post-germination. Both microbial inoculum and fertilizer

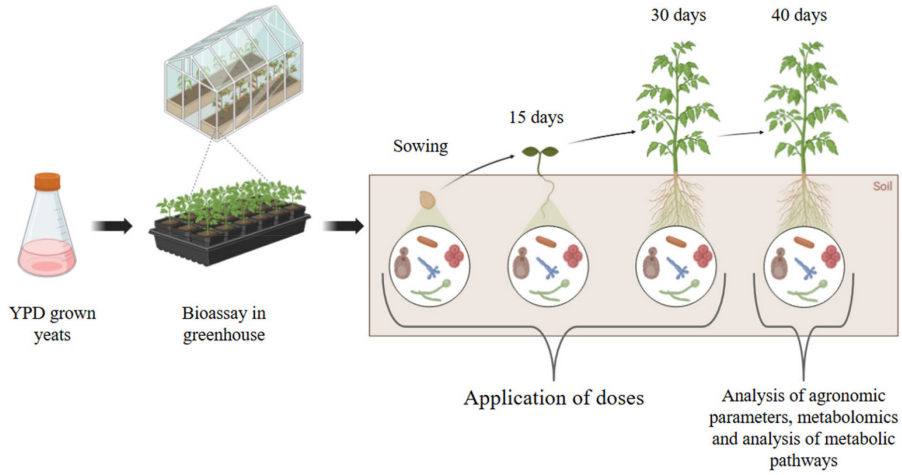

Figure 1. Schematic representation of the greenhouse bioassay designed to evaluate the plant growth-promoting effect of yeast strain L01 on tomato plants. Seedlings were grown in trays containing sterile commercial substrate and treated with L01AT and L01IN at a concentration of 1.11×10^9 CFU mL^{-1}. Three applications of 1 mL of yeast suspension were performed at germination, 15 days, and 30 days after sowing. At the same time, 3 mL of commercial fertilizer (NPK 8-8-8) was applied *per* plant. All experimental units were maintained in a greenhouse equipped with an automated irrigation system operating at 6:00 a.m., 10:00 a.m., 2:00 p.m., and 5:00 p.m., under controlled environmental conditions. Plants were cultivated for 40 days. This figure was created with Biorender (BioRender Inc., Canada, 2026).

were applied to the soil close to the root. The CF treatment received only the NPK fertilizer solution, without yeast inoculation.

The yeast strain, inoculation mode, and application dose were defined based on prior screening assays conducted by our research group. These assays demonstrated that applying of a suspension containing 10^9 CFU mL^{-1} *per* plant resulted in consistent growth responses. Higher concentrations caused phytotoxic effects and lower concentrations failed to elicit measurable responses. Accordingly, the inoculum concentration and application volume were selected to standardize microbial density in the rhizosphere across treatments.

All experimental units were kept in a greenhouse under an automated irrigation system (at 6:00 a.m., 10:00 a.m., 2:00 p.m. and 5:00 p.m.). Photoperiod was not controlled. The seedlings were collected approximately 40 days after sowing, when the roots completely filled the cells of the trays. To evaluate seedling quality, a scoring system was adopted in which each agronomic parameter received a score from 1 (least important) to 10 (most important). The scores assigned are shown in Table 1.[18]

Table 1. Score attributed to the classification of the most important parameters for the agronomic evaluation of seedlings

Agronomic parameter	Code	Score
Stem diameter	SD	1
Root length	RL	2
Plant height	H	3
Root fresh mass	RFM	4
Shoot fresh mas	AFM	5
Total fresh mass	TFM	6
Root dry mass	RDM	7
Shoot dry mass	ADM	8
Total dry mass	TDM	9
Dickson quality index	QDI	10

The variables were subjected to statistical analysis using analysis of variance (ANOVA) followed by the Tukey's test, with a significance level of 5%. If a significant difference was observed in relation to the control, the corresponding score was assigned to that parameter for that treatment. For example, the root fresh mass (RFM) parameter received a score of 4. If a treatment showed statistically significant differences from the control in terms of RFM, 4 points were added to the score of that treatment. Finally, the scores assigned to each parameter were summed for each treatment, and the treatments were ranked in descending order of score, thus determining the best performance compared to the control, which received no score.

Mass spectrometry-based metabolomics

Leaves were selected for metabolomic analysis because they synthesize and integrate a wide range of signals related to development, nutrition, and stress to regulate plant growth and survival.[19] Although yeast inoculation was applied to the rhizosphere, leaves are highly sensitive to systemic metabolic adjustments triggered by root-microorganism interactions.[20,21] Signals induced in the rhizosphere, including hormonal and metabolic stimuli, are translocated to aerial tissues via vascular transport and rapidly reflected in leaf metabolism.[21,22] As a result, leaves undergo pronounced metabolic reprogramming during growth, making them particularly suitable for detecting changes in primary and secondary metabolic pathways associated with plant growth promotion and stress responses.[23,24]

For metabolomic analysis, all leaves from each tomato seedling were collected and ground in liquid nitrogen prior to solvent extraction. The metabolomics analysis was performed using ultra-performance liquid chromatography coupled to tandem mass spectrometry (UHPLC-MS/MS), adapted from Rodrigues Neto *et al*.[25] The extraction of metabolites from tomato leaves was performed following the protocol described by de Souza *et al.*,[26] with adaptations. Approximately 100 mg of the sample were extracted with 500 µL of extraction solvent (methanol:water 8:2 v/v, ampicillin at 50 µg mL^{-1} and formic acid 0.1%). After homogenization, the samples were centrifuged and the supernatant collected and analyzed by UHPLC-MS/MS (maXis II Bruker™), equipped with an electrospray source (ESI), a quadrupole and high-resolution time-of-flight (Q-TOF) mass analyzer. Ampicillin was used as an internal standard in all chromatographic runs.

Reverse-phase liquid chromatography was used to separate the analytes, using an Acquity UPLC HSS T3 column (2.1 × 100 mm × 1.8 µm, Waters) at 35 °C. The solvents used in the mobile phase were: 0.1% formic acid (FA) in water (solvent A) and 0.1% formic acid in acetonitrile (solvent B). A flow rate of 400 µL min^{-1} was used.

The mass spectrometer was operated in positive (UHPLC-ESI(+)-MS/MS) and negative (UHPLC-ESI(–)-MS/MS) modes, configured at a capillary voltage of 3800 V, nebulizer pressure at 4.0 bar, drying gas at 9.0 L min^{-1} at 200 °C, cone temperature at 200 °C; column temperature at 40 °C; spectral acquisition rate of 3 Hz and monitored mass-to-charge ratio range (*m/z*) 80-1200 Dalton (Da). The equipment was calibrated with a sodium formate cluster (1 mM sodium formate in 10 mM NaOH, prepared in a 1:1 (v/v) isopropanol:water solution containing 0.2% formic acid), inserted directly at the beginning of each run.

Chemometric analysis

The data were processed using chemometric analysis. Data preprocessing was performed on the MZmine 3 online platform,[27,28] maintaining the information of (*i*) feature detection, (*ii*) retention time correction and (*iii*) alignment of retention times between samples.

Data were processed on the MetaboAnalyst 6.0 platform.[29] Chemometric methods, such as linear regression analysis combined with multidimensional analysis, partial least squares (PLS) analysis, were used for data processing. PLS is a supervised classification method that combines principal component analysis (PCA) with multiple linear regression to model variance within a dataset.[30-32] Partial least squares discriminant analysis (PLS-DA) modeling involves two procedures, the reduction of the dimension through the construction of PLS-DA components and the construction of a prediction model through discriminant analysis with the lowest possible error.[33,34] However, PLS analysis of metabolomic data is prone to overfitting, due to its complexity and the possibility of capturing noise along with the data, making validation necessary to estimate its predictive capacity.[35] Leave-one-out cross-validation (LOOCV) partitions the data, where an individual is removed from the model, while the remaining data generate another model.[35] This process is repeated so that each individual in the entire dataset is used only once for validation.[35] A validated standard error is calculated from the predictive sum.[36] LOOCV validation is accurate and offers almost unbiased error estimation, striking a balance between bias and variance, demonstrating robustness of the model.[35,37,38] A comparison test of scaling techniques was performed before the statistical tests. The scaling levels out the discrepant values of the variables in each sample, delimiting the differences in these variables. Two scaling methods were tested, auto scaling and Pareto scaling. In the comparison of the data using positive and negative ionization modes, the auto scaling proved to be more adequate due to the lower area usage in each component.

Metabolic pathway analysis and identification of compounds

Metabolic pathway analyses were performed using the pathway analysis module in the MetaboAnalyst 6.0 platform.[29] Comparisons were performed between CF tomato seedlings and seedlings treated with active (L01AT) and inactive (L01IN) yeast.

UHPLC-MS/MS data were used to perform pathway enrichment analysis and visual exploration based on the mummichog algorithm.[39] This algorithm predicts the functional activity of metabolites from high-resolution *m/z* peaks without requiring annotation and identification of each peak. In addition, it compares the number of overlapping metabolites with the number of corresponding *m/z* features and uses the smaller of these values for pathway enrichment calculations.

The interaction between the annotated compounds and their respective metabolic pathways was ranked in comparison with databases of the plant *Arabidopsis thaliana* plant databases, selected due to its physiological similarity to tomato, as both species are dicotyledons.

The raw data were first converted to .mzXML format using MSConvert software, version 3 (ProteoWizard Software Foundation, USA). The .mzXML files were submitted to MZmine 3 software, generating a .mgf file and a corresponding feature list. This data was submitted to the GNPS2 (Global Natural Product Social Molecular Networking 2)[40] platform for putative metabolite annotation, using the "librarysearch_workflow".

During processing, the data were filtered to remove MS/MS fragment ions located in the 1 Da range relative to the precursor ion (*m/z*). The mass tolerances for the precursor ion and for the fragment ions were set at 0.05 and 0.5 Da, respectively. Subsequently, the spectra were compared with the GNPS2 spectral libraries, applying the same filtering procedure to the reference data. Matches between spectra were considered acceptable when they presented a similarity score (cosine score) ≥ 0.7 and at least three shared peaks.

Finally, the annotated compounds were compared with the databases present in the GNPS spectral library for classification and putative assignment of metabolites.

Results and Discussion

Plant growth-promoting yeasts bioprospecting

To evaluate the effect of L01AT and L01IN treatments on tomato seedling growth, agronomic parameters were measured and subjected to statistical analysis. Statistical analysis was employed to compare yeast-inoculated plants with the control condition (CF) (Figure 2 and Table 2).

L01AT inoculation promoted tomato growth by increasing plant height (H), root fresh mass (RFM), and total fresh mass (TFM). On the other hand, L01IN inoculation perform an alteration on plant H, shoot fresh mass (AFM), RFM, TFM, shoot dry mass (ADM), root dry mass (RDM), total dry mass (TDM), and Dickson quality index (QDI). Although no significant difference was observed in the root length (RL) and stem diameter (SD) of tomato seedlings inoculated with L01AT and L01IN,

Figure 2. Tomato seedlings after inoculation of L01 in the active and inactive forms, L01AT and L01IN, respectively, compared to fertilizer control, CF.

both inoculants significantly increased plant growth and biomass compared to CF (Figure 2).

According to Table 2, the treatment using L01IN presented a higher score (52) when compared to L01AT (13), suggesting that the beneficial effects on plant growth are linked to the residual structural or metabolic components of the inactive yeast. The break of yeast cells releases intracellular nutrients, enriching the medium with organic nitrogen, amino acids, vitamins, and cell wall constituents. These compounds can function as a direct source of relatively fast-absorbing nutrients, benefiting plant nutrition.[41,42] In addition, the presence of living microorganisms in the host plant triggers a physiological state called "priming". After this activation, the plant responds more quickly and efficiently to subsequent pathogen invasions.[43,44] However, this inoculation can establish a dynamic of competition for both physical space (root, rhizosphere, leaf epidermis) and available resources (exuded sugars, amino acids, micronutrients).[45] Competition for available resources can temporarily reduce the availability of macro- and micronutrients through solubilization, siderophore production, or changes in local pH for the plant or other microorganisms, which will release metabolites that can hinder plant nutrition and development. For a deeper understanding, mass spectrometry-based metabolomics was used to study the metabolic interactions between PGPY and tomato seedling after two different inoculation treatments, using active and heat-inactive forms of L01.

Mass spectrometry-based metabolomics of plant growth-promoting yeasts

Mass spectrometry-based metabolomics was performed using a high resolution mass spectrometer with electrospray ionization in both modes, ESI(+)-MS/MS and ESI(–)-MS/MS. All analyses were performed comparing treated tomato leaves (L01AT and L01IN) with untreated tomato leaves (CF) 40 days after sowing. In the construction of the variable matrix, the peaks present in the "blank" were subtracted, considering the retention time (t_R) of 0.3-13 min. The chromatographic and mass spectral data were organized in a table with variables of interest, such as retention time and mass intensity. As the amount of metabolomic data generated is large, complex, and challenging to interpret concisely, chemometric methods were incorporated into the data processing.

Chemometric data processing

The metabolomic analysis of tomato seedling leaves treated with L01 yeast revealed consistent alterations in metabolic profiles for both the active (L01AT) and inactive (L01IN) forms when compared with the fertilizer control (CF).

For the L01AT treatment, multivariate analysis by PLS-DA applied to UHPLC-ESI(–)-MS/MS and UHPLC-ESI(+)-MS/MS datasets demonstrated a clear and reproducible separation between treated samples and

Table 2. Classification of *Sporidiobolus* (L01) yeast regarding growth and biomass parameters of tomato seedlings. L01AT contains viable cells of the yeast L01. L01IN contains dead cells resulting from autoclaving of the yeast L01. For classification, a score was assigned to the agronomic parameters according to their importance in seedling quality

	Treatment	Agronomic parameter										Total
		H	RL	SD	AFM	RFM	TFM	ADM	RDM	TDM	QDI	
01	L01IN											52
02	L01AT											13
03	CF											0

H: plant height (3); RL: root length (2); SD: stem diameter (1); AFM: shoot fresh mass (5); RFM: root fresh mass (4); TFM: total fresh mass (6); ADM: shoot dry mass (8); RDM: root dry mass (7); TDM: total dry mass (9); QDI: Dickson quality index (10).

the control, indicating a pronounced treatment-induced metabolic reprogramming. Replicates corresponding to leaves treated with L01AT are highlighted in green, whereas non-treated control leaves (CF) are represented separately, allowing visual distinction between the experimental groups. The cumulative explained variance reached 75.5% in the negative ionization mode and 79.9% in the positive mode, supporting adequate model performance (Figures 3a and 4a). Model robustness was assessed by LOOCV, yielding Q^2 values of 0.41 for ESI(–) and 0.46 for ESI(+), which are considered acceptable for untargeted metabolomics studies, as Q^2 values above 0.40 indicate adequate predictive ability in models with limited biological replication (Figures 3b and 4b). The hierarchical cluster dendrograms, constructed based on Ward's method and Euclidean distance corroborated these findings, showing high intragroup homogeneity and consistent segregation between L01AT and CF, particularly in the ESI(+) mode (Figures 3c and 4c). A minor deviation observed for a single replicate in the ESI(–) mode did not compromise the overall clustering pattern and was attributed to inherent biological variability among plant replicates.

For leaves treated with the inactive yeast (L01IN), PLS-DA also revealed a clear separation from the control in both ionization modes, indicating that non-viable yeast biomass retains the ability to modulate leaf metabolism. Replicates corresponding to leaves treated with L01IN are highlighted in green, whereas non-treated control leaves (CF) are represented separately, allowing visual distinction between the experimental groups. The explained variance reached 57.9% in the negative mode and 77.8% in the positive mode, reflecting statistically acceptable models, although with lower discriminatory power than those observed for L01AT (Figures 5a and 6a). LOOCV validation resulted in Q^2 values of 0.40 for ESI(–) and 0.43 for ESI(+), confirming acceptable predictive performance according to established metabolomics criteria (Figures 5b and 6b). However, hierarchical clustering revealed reduced intragroup homogeneity

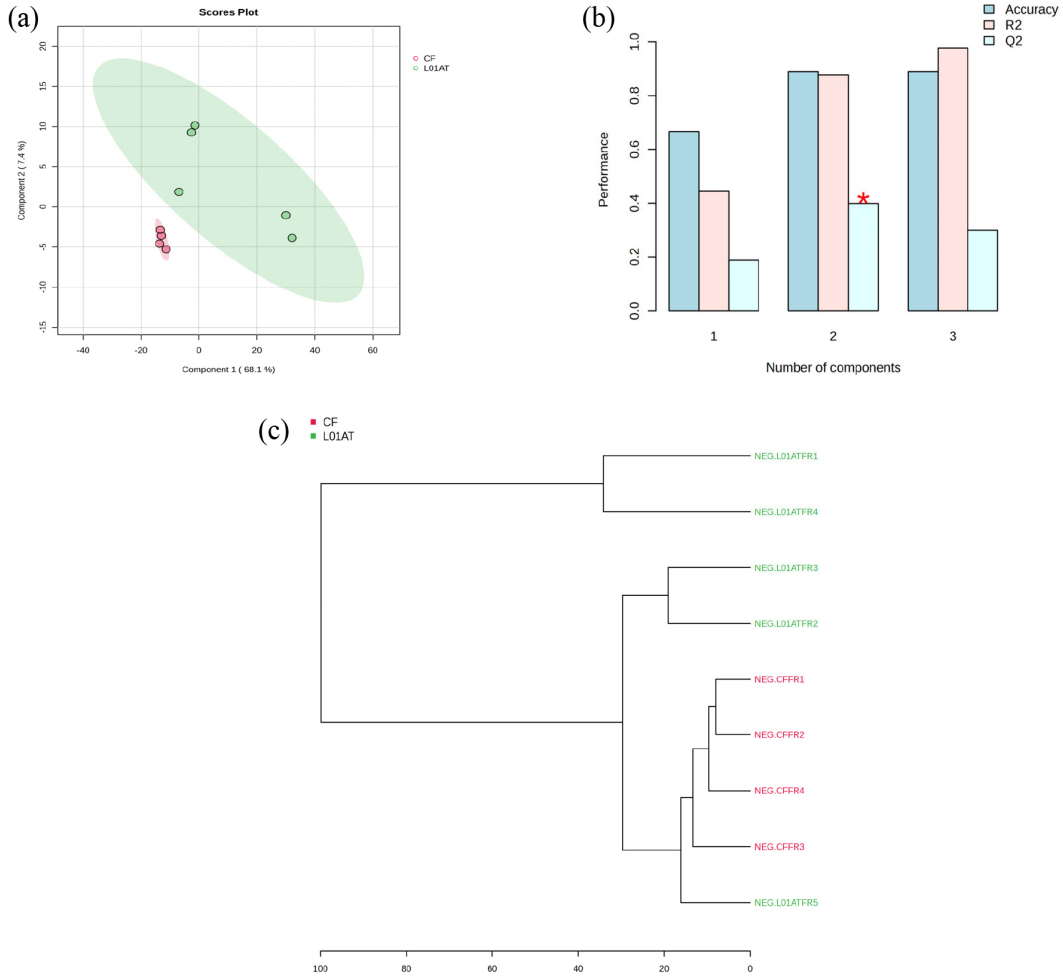

Figure 3. PLS-DA score graph (a), cross-validation (b) and hierarchical grouping dendrogram (c) for the visual representation of the distinct chemical profiles of the leaves of the CF *versus* L01AT using UHPLC-ESI(–)-MS/MS.

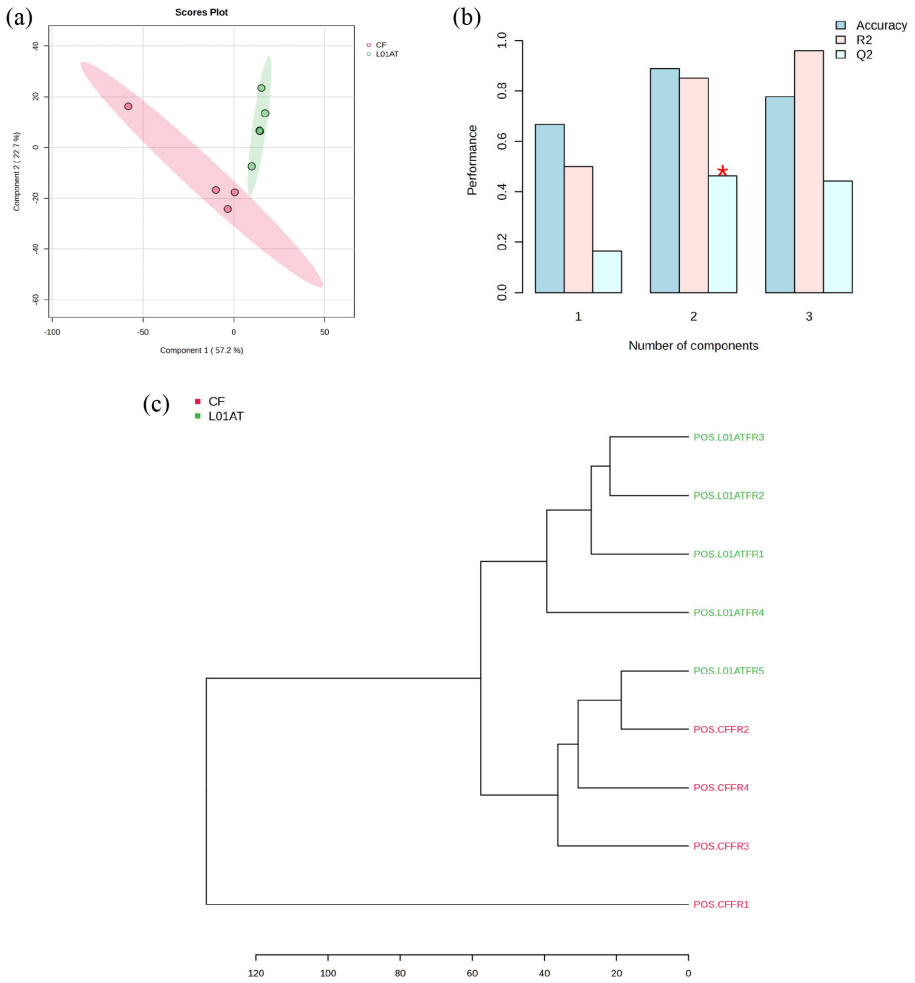

Figure 4. PLS-DA score graph (a), cross-validation (b) and hierarchical grouping dendrogram (c) for the visual representation of the distinct chemical profiles of the leaves of the CF *versus* L01AT using UHPLC-ESI(+)-MS/MS.

compared with L01AT, suggesting greater biological variability among replicates (Figures 5c and 6c). This pattern indicates that the metabolic effects of L01IN are likely mediated by structural components and residual metabolites rather than active microbial signaling.

A chemometric analysis was performed to compare the metabolic profile of treatments L01AT and L01IN (Figure 7). A clear difference between the samples is observed, indicating that although both treatments promote plant growth, the leaves of tomato seedlings produce a different metabolite profile after each form of inoculation. This behavior was observed in both ionization modes and reflected in the PLS-DA and hierarchical clustering plots (Figure 7). The high variance values indicate that the model is well-structured to discriminate between the two treatments. LOOCV validation indicated high predictive power, suggesting that the model has relevant classification capability. Hierarchical analysis using Ward's method with Euclidean distance reinforced the formation of two clusters consistent with the treatments, demonstrating that most replicates of L01AT and L01IN share a distinct metabolic pattern from the control (Figure 7). An outlier was identified that was closer to the CF group, a behavior that may be due to natural biological variation. These results indicate that inoculation with L01AT consistently modifies the leaf metabolome in most samples, pointing to the presence of differential metabolites that strongly contribute to the discrimination between groups and that deserve identification and enrichment of metabolic pathways to attribute functional significance to the observed changes. This observation is expected, as the metabolic composition of the inoculum changes after heating (inactive form), consequently altering its interaction with the plant.

The chemometric analysis showed a separation between the groups: (1) L01AT *versus* CF, (2) L01IN *vs.* CF, and (3) L01IN *vs.* L01AT, indicating that both the active and inactive forms of the L01 strain cause changes in the metabolic profile of tomato seedlings comparing to the fertilizer. This supports the hypothesis that the plant/

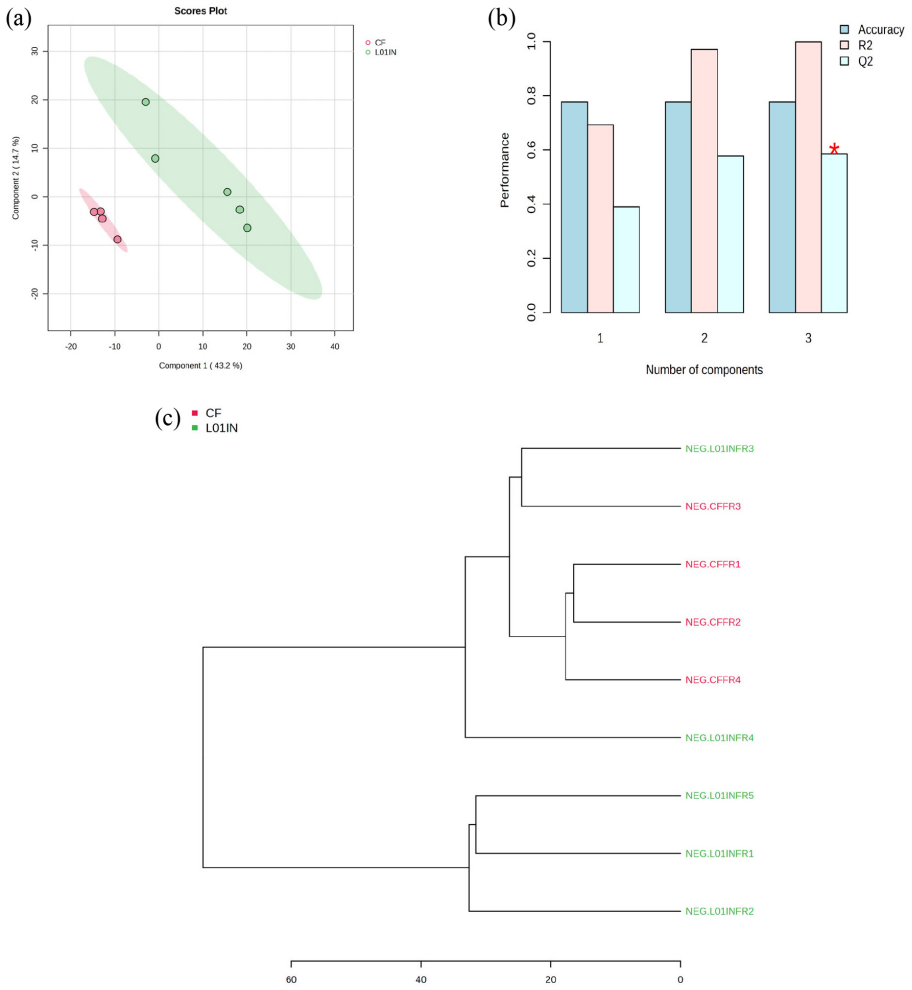

Figure 5. PLS-DA score graph (a), cross-validation (b) and hierarchical grouping dendrogram (c) for the visual representation of the distinct chemical profiles of the leaves of the CF *versus* L01IN using UHPLC-ESI(–)-MS/MS.

microorganism interaction can modulate and alter the metabolic profile of the plant. However, to gain a deeper understanding, we carried out an analysis of metabolic pathways and identified the most important metabolites of tomato seedling leaves.

Metabolite and metabolic pathway annotation

The metabolic pathways activated in the leaves of the seedlings treated with the yeast L01 were evaluated through the enrichment analysis and topological pathway mapping. The enrichment analysis and topological metabolic pathways graph depict the set of metabolic pathways in two dimensions, where the x-axis represents the impact of the metabolic pathway in the topological analysis. This value is calculated by summing the importance measures of each corresponding metabolite and dividing by the total of the importance measures of all metabolites in each pathway. The y-axis, on the other hand, represents the negative logarithm of the *p*-value, indicating the probability of observing the concentration or presence of metabolites in a specific pathway by chance, given the characteristics of the analyzed dataset.

The comparison between CF and treatment (L01AT and L01IN) can be seen in Figure 8. The five metabolic pathways were found to be statistically relevant in the leaves treated with the L01AT and L01IN, compared with the CF, are presented in Table 3.

The following metabolic pathways were activated in tomato seedling leaves after L01AT: (*i*) biosynthesis of phenylpropanoids (*ii*) biosynthesis of flavones and flavonols (*iii*) biosynthesis of anthocyanins (*iv*) biosynthesis of cutin, suberin and wax (*v*) biosynthesis of phenylalanine, tyrosine and tryptophan.

(*i*) The phenylpropanoid biosynthesis pathway comprises several metabolites required for lignin biosynthesis and includes important compounds such as flavonoids, coumarins and lignans.[46] This pathway plays an important role in strengthening the plant cell wall (lignification), increases mechanical strength, and

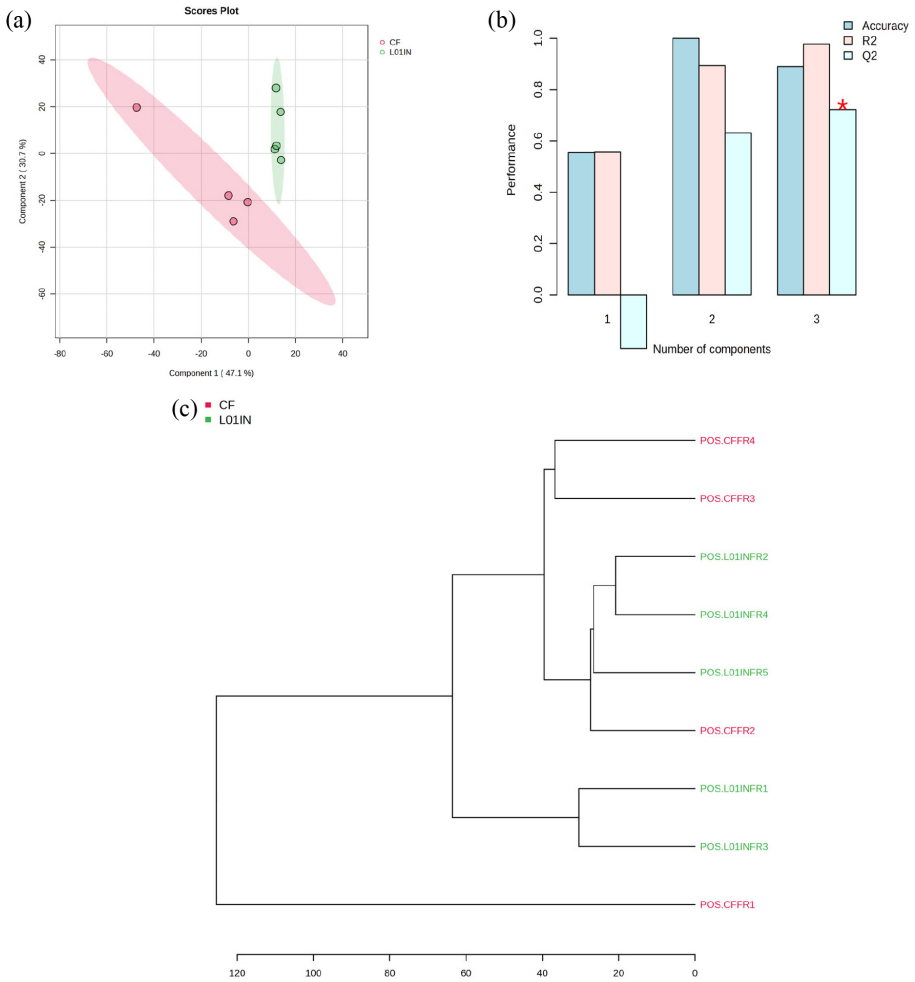

Figure 6. PLS-DA score graph (a), cross-validation (b) and hierarchical grouping dendrogram (c) for the visual representation of the distinct chemical profiles of the leaves of the CF *versus* L01IN using UHPLC-ESI(+)-MS/MS,

participates in defense against pathogens and environmental stresses (ultraviolet, metals, and drought).[46-48] The activation of this pathway indicates that the plant is redirecting carbon from primary to secondary metabolism in order to synthesize compounds with structural and defense functions. In the leaves of tomato seedlings treated with the yeast L01 in the active form (L01AT), the compounds 1-[4-hydroxy-3-(3-methylbut-2-enyl)phenyl]ethanone, 3-*p*-coumaroylquinic acid, cryptochlorogenic acid and *p*-coumaric acid (*p*-CA) were identified. The compound *p*-CA is synthesized from tyrosine and phenylalanine via the shikimate metabolic pathway and represents a key metabolic link between aromatic amino acid biosynthesis and phenylpropanoid-derived defense compounds.[47] These metabolites are involved in plant defense, structural support and survival, mediating responses to abiotic (ultraviolet radiation, cold, salt, drought and heavy metals) and biotic (herbivores, bacteria, fungi) stresses.[48,49]

(*ii*) Flavonoids represent a major class of plant secondary metabolites and are important antioxidants and signaling molecules in plant defense.[50,51] These compounds are synthesized through the phenylpropanoid metabolic pathway and include flavonoids such as quercetin, kaempferol, roseoside and rutin, all of which were identified in L01AT-treated leaves.[52] These flavonoids act as potent antioxidants, contributing to reactive oxygen species scavenging, participate in defense mechanisms, protection against ultraviolet radiation, and modulation of phytohormone signaling.[52,53] By reinforcing the endogenous antioxidant system, flavonoids enhance plant resilience under both biotic and abiotic stress conditions, indirectly supporting sustained growth and physiological stability.[53]

(*iii*) Anthocyanins (biosynthesis of anthocyanins) are a subclass of flavonoids that function as natural pigments and are typically synthesized under stress conditions or pathogen attack.[53] The activation of the anthocyanin biosynthesis pathway without the detection of metabolites can be explained by the regulatory dynamics of phenylpropanoid-derived metabolism. The accumulation

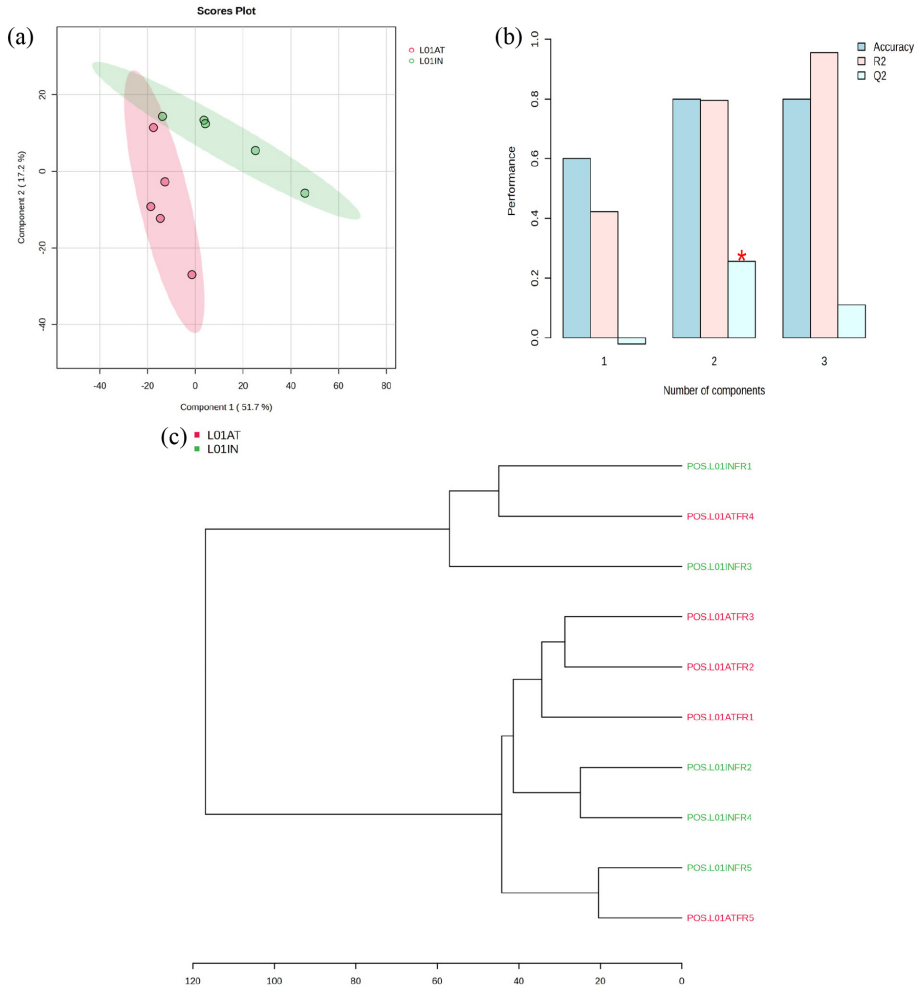

Figure 7. PLS-DA score graph (a), cross-validation (b) and hierarchical grouping dendrogram (c) for the visual representation of the distinct chemical profiles of the leaves of the L01AT *versus* L01IN using and UHPLC-ESI(+)-MS/MS,

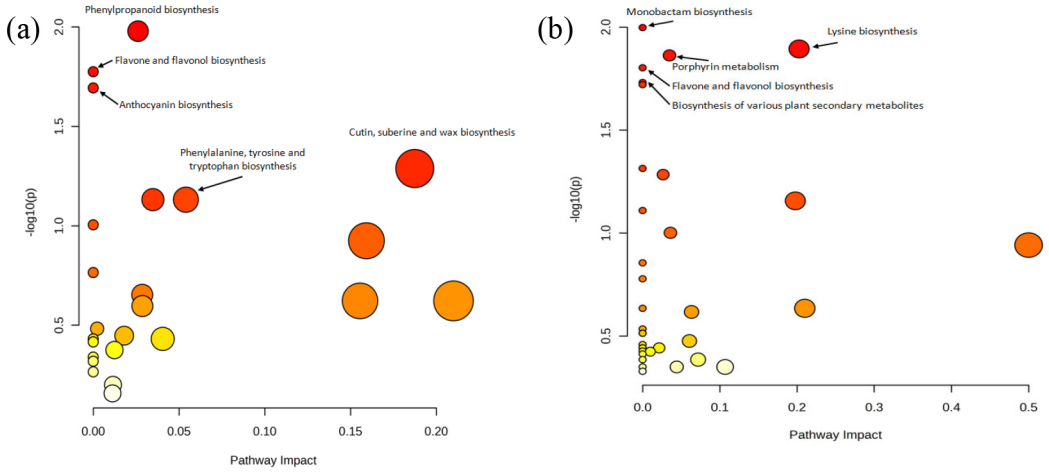

Figure 8. Enrichment and topological analysis of metabolic pathways of tomato seedling leaves after inoculation of (a) L01AT and (b) L01IN compared to the control. Each dot represents a metabolic pathway. Size indicates the impact of the pathway, and color indicates statistical significance (from yellow to red, with red being the most significant). Pathways at the top right are the most relevant, as they have both high impact and high significance.

of metabolites, including phenylalanine and *p*-coumaric acid, along with the presence of flavonols such as rutin, quercetin, and kaempferol derivatives, indicates that the metabolic flux was intensified towards the biosynthesis of phenylpropanoids and flavonoids, but did not progress towards the accumulation of anthocyanins.

Table 3. Metabolic pathways activated in tomato seedling leaves after L01AT and L01IN inoculation

Sample	Metabolic pathway	Classification
L01AT	phenylpropanoid biosynthesis	secondary metabolism
	flavone and flavonol biosynthesis	secondary metabolism
	anthocyanin biosynthesis	secondary metabolism
	cutin, suberin and wax biosynthesis	primary metabolism
	phenylalanine, tyrosine and tryptophan biosynthesis	primary metabolism
L01IN	monobactam biosynthesis	secondary metabolism
	lysine biosynthesis	primary metabolism
	porphyrin metabolism	primary metabolism
	flavone and flavonol biosynthesis	secondary metabolism
	biosynthesis of various plant secondary metabolites	secondary metabolism

(*iv*) The activation of the biosynthesis pathway of cutin, suberin and wax are related to the formation and remodeling of extracellular protective barriers. This pathway contributes to cuticle reinforcement and the development of outer leaf structures that reduce water loss and limit pathogen entry. Its activation in L01AT-treated leaves indicates that yeast application induces structural adaptations resulting in enhanced tissue protection, improved waterproofing of the polysaccharide-based cell walls and increased tolerance to environmental stress.[54,55]

(*v*) Phenylalanine, tyrosine, and tryptophan are aromatic amino acids essential for protein synthesis and development.[56,57] Beyond their role as proteinogenic amino acids, these compounds serve as key precursors for the biosynthesis of phytohormones, phenolic polymers, alkaloids and lignin.[56-58] This pathway is considered an intermediate metabolic route and is tightly linked to the phenylpropanoid biosynthesis.[58] The identification of quinic acid ((1*S*,3*R*,4*S*,5*R*)-1,3,4,5-tetrahydroxycyclohexane-1-carboxylic), a shikimate pathway intermediate, highlights the metabolic connection between central carbon metabolism and aromatic amino acid biosynthesis.[59-61] In addition, the presence of quinic acid suggests enhanced allocation of photosynthetic fixed carbon toward secondary metabolite production via phenylalanine derived pathways, reinforcing defense-related metabolism.[62]

The use of L01AT yeast tends to induce secondary pathways linked to defense and environmental adaptation. This pattern is consistent with a priming effect or defensive stimulus through the plant/living microorganism interaction, where the plant prepares defense metabolisms and increases phenol/flavonoid biosynthesis. This activation indicates that the living microorganism triggers defense, antioxidant, and structural responses. This characterizes the biostimulation effect associated with the induction of systemic resistance, a phenomenon typical of plant PGPYs.

The following metabolic pathways were activated in tomato seedling leaves after L01IN: (*i*) monobactams biosynthesis, (*ii*) lysine biosynthesis, (*iii*) porphyrin metabolism, (*iv*) flavone and flavonol biosynthesis, and (*v*) biosynthesis of several plant secondary metabolites.

(*i*) Biosynthesis of monobactama belongs to secondary metabolism and includes a group of naturally occurring antibiotics effective against Gram-negative bacteria. The activation of this pathway suggests an indirect modulation of plant-microorganism interactions, potentially contributing to microbial balance and pathogen suppression.

(*ii*) The lysine biosynthesis pathway, although part of primary metabolism, can be used for the synthesis of pipecolic acid.[63,64] Pipecolic acid is an important non-proteinogenic amino acid that plays a role in plant defense signaling and metabolic regulation.[63,64] It acts as a signaling molecule and precursor of secondary metabolites, including alkaloids and other nitrogenous compounds.[63,64] There are several pathways as well as specific enzymes involved in some catalytic steps in the conversion of L-lysine to pipecolic acid. Some pathways may provide pipecolic acid for the biosynthesis of specific secondary metabolites, others may only accumulate this amino acid as an intermediate or derivative product of a primary metabolic pathway. Despite the identification of lysine and pipecolic acid in the leaves of seedlings treated with L01IN, additional studies are needed to provide complete information on which biosynthesis route is being used.

(*iii*) The porphyrin metabolism pathway, present in primary metabolism, describes the synthesis and breakdown of porphyrin. Porphyrins are compounds that have important functions in light absorption and vital processes like respiration and photosynthesis.[65] They include heme, chlorophyll, vitamin B12, bilin, and coenzyme F430. Although they are activated in leaves that were treated with L01IN, when compared with CF,

no metabolites of the porphyrin metabolism pathway were identified. This suggests that the observed activation likely reflects the regulation of photosynthetic and energy metabolism, rather than the accumulation of porphyrin end products, possibly contributing to improved physiological performance and growth.

(*iv*) The flavone and flavonol biosynthesis pathway was also activated in L01IN-treated leaves. Flavonoids such as delphinidine 3-galactoside, kaempferol 3-*O*-rutinoside and rutin were identified. These are responsible for signaling and responding to abiotic (ultraviolet radiation, cold, salt, drought, and heavy metal) and biotic (herbivores, bacteria, fungi) stresses.[66] In addition to their defensive functions, these flavonoids act as antioxidants and modulators of hormone signaling, indirectly supporting plant growth and physiological stability.[66]

(*v*) The biosynthetic pathway of several secondary plant metabolites was activated due to the high diversity and abundance of annotated secondary metabolites. This pathway represents an integrative metabolic network linking primary metabolism to specialized defense and adaptation processes. In addition, they play crucial roles in stress adaptation and in various physiological functions, making them essential for plant survival and defense. Among the secondary metabolites identified, the most important were: (*R*)-linalyl beta-vicianoside, acanthoside B, furostan, harpagide, solasodine and tomatidine. These compounds are related to defense, stress tolerance, and growth regulation in tomatoes. In addition, these metabolites indicate the adaptive capacity of the plant.

Treatment with L01IN preferentially activated pathways associated with nitrogen assimilation, amino acid biosynthesis, pigment metabolism, and energy-related processes. This pattern suggests that the inactivated yeast biomass is metabolized by the plant as an organic nutrient source, supplying nitrogen, carbon skeletons, and signaling molecules that support growth-related pathways.

A detailed list containing the most important compounds assigned using UHPLC-ESI(–/+)-MS/MS is presented here. A total of 73 metabolites were annotated, being 36 and 37 metabolites detected in tomato seedling leaves treated with L01AT (Table 4) and L01IN (Table 5), respectively.

Metabolomic analysis of tomato seedling leaves demonstrated that yeast application alters metabolism, depending on yeast cell viability. Although treatments with L01AT and L01IN affected central metabolic pathways, the intensity of the alterations and the metabolic profile differed, as summarized in Figure 9.

Leaves treated with L01AT exhibited a metabolic profile marked by the accumulation of secondary metabolites, phenylpropanoids, flavonoids, alkaloids, terpenoids, and lipid-derived signaling molecules (Figure 9). This response was accompanied by alterations in important primary and secondary metabolites, such as phenylalanine, coumaric acid, roseoside, quercetin-4'-*O*-glucoside, and 5,6-epoxy-8*Z*,11*Z*,14*Z*-eicosatrienoic acid, indicating a coordinated reprogramming between primary and secondary metabolism. The induction of cryptochlorogenic acid and tomatidine further reinforces the activation of antioxidant processes, related to defense and growth regulation, consistent with an optimized metabolic state that increases physiological readiness without major energy penalties.

In contrast, leaves treated with L01IN showed a metabolomic profile dominated by primary metabolic intermediates, including organic acids, amino acids, carbohydrates, nucleotides, and lipids (Figure 9). The predominance of metabolites such as quinic acid, isocitric acid, rutinose, curcumin, and furostan indicates an overall metabolic adjustment focused on energy balance, structural maintenance, and redox homeostasis, with limited engagement of specialized metabolic pathways.

These results highlight the importance of selecting the appropriate yeast application method, since each treatment triggers distinct metabolic responses. The strategic use of active or inactive yeasts can direct the plant towards specific growth, nutrition, or resistance responses, representing a promising biotechnological tool for the physiological and metabolic management of tomato plants. Therefore, the differentiated metabolic responses induced by active and inactivated yeast biomass highlight the potential of customized bioinput strategies capable of optimizing plant performance, maintaining metabolic resilience, and reinforcing the applicability of these systems in sustainable agriculture based on chemical principles.

Conclusions

In this study, a comprehensive analysis, integrating agronomic, biological, and chemical data offered a detailed view of the metabolic alterations induced by PGPY in tomato seedling. Both active (L01AT) and heat-inactivated (L01IN) yeast inoculation forms promoted the growth of tomato seedlings and induced distinct, yet consistent, changes in the leaf metabolic profile, demonstrating that yeast-derived bioinputs can act as effective metabolic modulators. Untargeted metabolomics revealed extensive metabolic reprogramming, with amino acid-related pathways emerging as central components of primary metabolism and flavonoid-related pathways as key hubs of secondary metabolism.

Table 4. Chemical composition of tomato seedlings leaves after inoculation of yeast L01AT

Compound name	Molecular formula	Adduct	*m/z*	Mass difference	Cosine	Retention time / min	Classification
Quinate	$C_7H_{12}O_6$	$[M - H]^-$	191.056	0.0003	0.938	0.652	primary/organic acids
Citric acid	$C_6H_{11}NO_7$	$[M + H]^+$	210.061	0.0012	0.760	0.864	primary/organic acids
Pipecolic acid	$C_6H_{11}NO_2$	$[M + H]^+$	130.05	0.036	0.933	0.609	primary/amino acid
Arginine	$C_6H_{14}N_4O_2$	$[M + H]^+$	175.119	0.000	0.754	0.533	primary/amino acid
Phenylalanine	$C_9H_{11}NO_2$	$[M + H]^+$	166.086	0.000	0.906	2.002	primary/amino acid
Glutamine	$C_5H_{10}N_2O_3$	$[2M + H]^+$	293.146	0.001	0.732	0.595	primary/amino acid
Lysine	$C_6H_{14}N_2O_2$	$[M + H]^+$	147.076	0.037	0.964	0.595	primary/amino acid
Tyrosine	$C_9H_{12}NO_3$	$[M + H]^+$	182.081	0.000	0.983	0.972	primary/amino acid
Trehalose	$C_{17}H_{30}O_{15}$	$[M - H_2O + H]^+$	457.156	0.001	0.774	6.264	primary/ carbohydrates
Sucrose	$C_{12}H_{22}O_{11}$	$[M + NH_4]^+$	360.149	0.001	0.914	0.618	primary/ carbohydrates
5,6-Epoxy-8*Z*,11*Z*,14*Z*-eicosatrienoic acid	$C_{25}H_{47}NO$	$[M - H_2O + H]^+$	304.301	0.000	0.777	10.159	primary/lipids
Heptadecasfing-4-enine	$C_{21}H_{42}N_2O_3$	$[M + H]^+$	371.328	0.000	0.865	9.543	primary/lipids
Lyso-PC(16:0)	$C_{26}H_{48}NO_7P$	$[M + H]^+$	518.325	0.001	0.750	9.737	primary/lipids
1-Stearoyl-2-hydroxy-sn-glycero-3-phosphoethanolamine	$C_{23}H_{44}NO_7P$	$[M + H]^+$	478.295	0.002	0.781	10.416	primary/lipids
1-Palmitoyl-2-hydroxy-sn-glycero-3-phosphoethanolamine	$C_{39}H_{40}O_4$	$[M + H]^+$	573.305	0.002	0.808	10.949	primary/nucleotide
Adenine	$C_5H_5N_5$	$[M + H]^+$	136.062	0.000	0.817	0.655	secondary/ carboxylic acid
Coumaroylquinic acid	$C_{16}H_{18}O_8$	$[M + H]^+$	339.107	0.000	0.838	4.778	secondary/ alkaloids
Tyramine	$C_8H_{11}NO$	$[M + H–NH_3]^+$	121.064	0.001	0.738	1.126	secondary/ alkaloids
Solasodine	$C_{27}H_{45}NO_2$	$[M + H]^+$	416.354	0.002	0.833	6.264	secondary/ alkaloids
Tomatidine	$C_{33}H_{55}NO_7$	$[M + H]^+$	578.408	0.003	0.916	6.254	secondary/ phenolic compounds
1-[4-Hydroxy-3-(3-methylbut-2-enyl)phenyl] ethanone	$C_{13}H_{16}O_2$	$[M + H]^+$	205.086	0.036	0.845	11.811	secondary/ phenolic compounds
2-(3,4-Dihydroxyphenyl)-5-hydroxy-7-[(2*S*,3*R*,4*S*,5*S*,6*R*)-3,4,5-trihydroxy-6-[[(2*R*,3*R*,4*R*,5*R*,6*S*)-3,4,5-trihydroxy-6-methyloxan-2-yl]oxymethyl]oxan-2-yl] oxychromen-4-one	$C_{27}H_{30}O_{15}$	$[M + H]^+$	595.166	0.001	0.976	5.415	secondary/ phenolic compounds
2-(3,4-Dihydroxyphenyl)-5,7-dihydroxy-3-(((2*S*,3*R*,4*S*,5*S*,6*R*)-3,4,5-trihydroxy-6-((((3*R*,4*R*,5*R*,6*S*)-3,4,5 -trihydroxy-6-methyltetrahydro-2*H*-pyran-2-yl)oxy)methyl) tetrahydro-2*H*-pyran-2-yl)oxy)-4*H*-chromen-4-one	$C_{27}H_{30}O_{16}$	$[M + Na]^+$	633.143	0.003	0.851	5.118	secondary/ phenolic compounds

Table 4. Chemical composition of tomato seedlings leaves after inoculation of yeast L01AT (cont.)

Compound name	Molecular formula	Adduct	*m/z*	Mass difference	Cosine	Retention time / min	Classification
2-(Hydroxymethyl)-6-[4-[(2*S*,3*S*)-3-(hydroxymethyl)-5-[(*E*)-3-hydroxyprop-1-enyl]-7-methoxy-2,3-dihydro-1-benzofuran-2-yl]-2-methoxyphenoxy]oxane-3,4,5-triol	$C_{26}H_{32}O_{11}$	$[M + NH_4]^+$	538.229	0.001	0.746	5.224	secondary/ compounds phenolics
3-[(2*S*,3*R*,4*S*,5*S*,6*R*)-6-[[(2*R*,3*R*,4*R*,5*R*,6*S*)-3-[(2*S*,3*R*,4*R*)-3,4-Dihydroxy-4-(hydroxymethyl)oxolan-2-yl] oxy-4,5-dihydroxy-6-methyloxan-2-yl] oxymethyl]-3,4,5-trihydroxyoxan-2-yl]oxy-2-(3,4-dihydroxyphenyl)-5,7-dihydroxychromen-4-one	$C_{32}H_{38}O_{20}$	$[M + H]^+$	743.206	0.003	0.874	4.854	secondary/ phenolic compounds
3-[4,5-Dihydroxy-6-(hydroxymethyl)-3-[(2*S*,3*R*,4*R*,5*R*,6*S*)-3,4,5-trihydroxy-6-methyloxan-2-yl]oxyoxan-2-yl] oxy-5-hydroxy-2-(4-hydroxyphenyl)-7-[3,4,5-trihydroxy-6-(hydroxymethyl)oxan-2-yl] oxychromen-4-one	$C_{33}H_{40}O_{20}$	$[M + H]^+$	757.223	0.005	0.822	4.382	secondary/ phenolic compounds
(*E*)-3-[4-[(2*S*,3*R*,4*S*,5*S*,6*R*)-3,4,5-Trihydroxy-6-(hydroxymethyl)oxan-2-yl]oxyphenyl] prop-2-enoic acid	$C_{15}H_{18}O_8$	$[M + NH_4]^+$	344.134	0.000	0.846	4.219	secondary/ phenolic compounds
Cryptochlorogenic acid	$C_{16}H_{18}O_9$	$[M + H]^+$	355.103	0.000	0.954	4.178	secondary/ phenolic compounds
Coumaric acid	$C_9H_8O_3$	$[M + H]^+$	165.054	0.001	0.843	4.222	secondary/ phenolic compounds
Furostane base + *O*-Hex, *O*-Hex-Hex-Hex	$C_{46}H_{81}N_7O_{20}$	$[M - H_2O + H]^+$	1034.56	0.008	0.866	6.236	secondary/ phenolic compounds
Kaempferol-3-*O*-rutinoside	$C_{27}H_{30}O_{15}$	$[M - H]^-$	593.152	0.0477	0.932	5.436	secondary/ phenolic compounds
Quercetin-4'-*O*-glucoside	$C_{21}H_{20}O_{12}$	$[M + H]^+$	465.103	0.000	0.846	5.118	secondary/ phenolic compounds
Roseoside	$C_{19}H_{30}O_8$	$[M + H]^+$	387.201	0.002	0.733	4.742	secondary/ phenolic compounds
Routine	$C_{27}H_{30}O_{16}$	$[M - H]^-$	609.147	0.0013	0.995	5.137	secondary/ phenolic compounds
4-[(*E*)-3-[(2*R*,3*R*,4*S*,5*S*,6*R*)-3-[(2*S*,3*R*,4*R*)-3,4-Dihydroxy-4-(hydroxymethyl)oxolan-2-yl] oxy-4,5-dihydroxy-6-(hydroxymethyl)oxan-2-yl]oxybut-1-enyl]-3,5,5-trimethylcyclohex-2-en-1-one	$C_{22}H_{32}O_{10}$	$[M + H]^+$	457.207	0.002	0.721	6.092	secondary/ terpenoids
Canrenone	$C_{13}H_{30}NO_5S$	$[M - H]^-$	311.168	0.0105	0.899	11.341	secondary/ terpenoids

The indicated stereochemistry for the compounds, as well as the positions of the functional groups and the specific isomerism, is based on the greater occurrence of these compounds in nature, in studies with structural characterizations and access to databases. However, this does not exclude the existence of other isomers, especially considering that high-resolution techniques still face limitations in differentiating chiral centers in complex samples such as plant extracts and microorganisms.

Table 5. Chemical composition of tomato seedlings leaves after inoculation of yeast L01IN

Compound name	Molecular formula	Adduct	*m/z*	Mass difference	Cosine	Retention time / min	Classification
Citric acid	$C_6H_8O_7$	$[M - H]^-$	191.02	0.0151	0.958	0.888	primary/organic acids
Isocitric acid	$C_6H_8O_7$	$[M + H]^+$	224.129	0.001	0.743	3.54	primary/organic acids
Quinic acid	$C_7H_{12}O_6$	$[M - H]^-$	191.056	0	0.963	0.647	primary/organic acids
Pipecolic acid	$C_6H_{11}NO_2$	$[M + H]^+$	130.05	0.036	0.918	0.6	primary/amino acids
Arginine	$C_6H_{14}N_4O_2$	$[M + H]^+$	175.118	0.001	0.752	0.55	primary/amino acids
Glutamine	$C_5H_{10}N_2O_3$	$[2M + H]^+$	293.146	0.001	0.836	0.577	primary/amino acids
Lysine	$C_6H_{14}N_2O_2$	$[M + H]^+$	147.076	0.037	0.941	0.605	primary/amino acids
Tyrosine	$C_9H_{11}NO_3$	$[M + H]^+$	182.081	0.004	0.805	0.989	primary/amino acids
Myristamidopropyl betaine	$C_{19}H_{38}N_2O_3$	$[M + H]^+$	343.296	0	0.903	8.461	primary/amino acids
Alpha-galactose 1-phosphate	$C_6H_{13}O_9P$	$[M - H]^-$	259.022	0	0.954	0.589	primary/ carbohydrates
Trehalose	$C_{17}H_{30}O_{15}$	$[M - H_2O + H]^+$	457.155	0.002	0.788	6.262	primary/ carbohydrates
Rutinose	$C_{11}H_{20}O_{10}$	$[M - H_2O + H]^+$	295.102	0.001	0.855	6.262	primary/ carbohydrates
Sucrose	$C_{12}H_{22}O_{11}$	$[M + NH_4]^+$	360.15	0	0.926	0.618	primary/ carbohydrates
Heptadecasfing-4-enina	$C_{21}H_{42}N_2O_3$	$[M + H]^+$	371.327	0.001	0.865	9.552	primary/lipids
Adenine	$C_5H_5N_5$	$[M + H]^+$	136.062	0	0.751	0.665	primary/ nucleotides
Adenosine	$C_{10}H_{13}N_5O_4$	$[M + H]^+$	268.104	0	0.94	1.013	primary/ nucleotides
N-Methylnicotinate	$C_7H_7NO_2$	$[M + H]^+$	138.055	0	0.93	0.618	secondary/ alkaloids
Solasodine	$C_{27}H_{45}NO_2$	$[M + H]^+$	416.353	0	0.851	6.262	secondary/ alkaloids
Tomatidine	$C_{33}H_{55}NO_7$	$[M + H]^+$	578.407	0.002	0.913	6.262	secondary/ alkaloids
Acanthoside B	$C_{28}H_{36}O_{13}$	$[M + NH_4]^+$	598.249	0	0.829	5.648	secondary/ phenolic compounds
(*E*)-3-[4-[(2*S*,3*R*,4*S*,5*S*,6*R*)-3,4,5-Trihydroxy-6-(hydroxymethyl)oxan-2-yl]oxyphenyl] prop-2-enoic acid	$C_{15}H_{18}O_8$	$[M + NH_4]^+$	344.134	0	0.811	4.225	secondary/ phenolic compounds
Curcumin	$C_{16}H_{18}O_9$	$[M + H]^+$	355.101	0.001	0.921	4.178	secondary/ phenolic compounds
Delphinidin 3-galactoside	$C_{21}H_{21}ClO_{12}$	$[M + Cl]^-$	465.102	0	0.857	5.135	secondary/ phenolic compounds
2-(3,4-Dihydroxyphenyl)-5-hydroxy-7-[(2*S*,3*R*,4*S*,5*S*,6*R*)-3,4,5-trihydroxy-6-[[(2*R*,3*R*,4*R*,5*R*,6*S*)-3,4,5-trihydroxy-6-methyloxan-2-yl]oxymethyl]oxan-2-yl] oxychromene-4-one	$C_{27}H_{30}O_{15}$	$[M + H]^+$	595.166	0.001	0.946	5.439	secondary/ phenolic compounds

Table 5. Chemical composition of tomato seedlings leaves after inoculation of yeast L01IN (cont.)

Compound name	Molecular formula	Adduct	*m/z*	Mass difference	Cosine	Retention time / min	Classification
2-(Hydroxymethyl)-6-[4-[(2*S*,3*S*)-3-(hydroxymethyl)-5-[(*E*)-3-hydroxy prop-1-enyl]-7-methoxy-2,3-dihydro-1-benzofuran-2-yl]-2-methoxyphenoxy]oxane-3,4,5-triol	$C_{26}H_{32}O_{11}$	$[M + NH_4]^+$	538.228	0	0.784	5.227	secondary/ phenolic compounds
3-[(2*S*,3*R*,4*S*,5*S*,6*R*)-6-[[(2*R*,3*R*,4*R*,5*R*,6*S*)-3-[(2*S*,3*R*,4*R*)-3,4-Dihydroxy-4-(hydroxymethyl)oxolan-2-yl]oxy-4,5-dihydroxy-6-methyloxan-2-yl]oxymethyl]-3,4,5-trihydroxyoxan-2-yl]oxy-2-(3,4-dihydroxyphenyl)-5,7-dihydroxychromen-4-one	$C_{32}H_{38}O_{20}$	$[M + H]^+$	743.201	0.002	0.844	4.874	secondary/ phenolic compounds
3-*O*-Feruloylquinic acid	$C_{17}H_{20}O_9$	$[M - H]^-$	367.103	0.0002	0.843	4.887	secondary/ phenolic compounds
Coumaroylquinic acid	$C_{16}H_{18}O_8$	$[M - H]^-$	337.093	0.0007	0.8855	4.665	secondary/ phenolic compounds
Kaempferol 3-*O*-rutinoside	$C_{32}H_{38}O_{19}$	$[M + H]^+$	727.209	0.001	0.869	5.089	secondary/ phenolic compounds
Kaempferol-3-glucoside-3”-rhamnoside	$C_{27}H_{30}O_{15}$	$[M + H]^+$	593.151	0	0.965	5.433	secondary/ phenolic compounds
Routine	$C_{27}H_{30}O_{16}$	$[M - H]^-$	609.147	0.001	0.982	5.141	secondary/ phenolic compounds
3-[4,5-Dihydroxy-6-(hydroxymethyl)-3-[(2*S*,3*R*,4*R*,5*R*,6*S*)-3,4,5-trihydroxy-6-methyloxan-2-yl]oxyoxan-2-yl]oxy-5-hydroxy-2-(4-hydroxyphenyl)-7-[3,4,5-trihydroxy-6-(hydroxymethyl)oxan-2-yl]oxychromen-4-one	$C_{45}H_{44}O_{19}$	$[M + H]^+$	889.252	0.009	0.784	4.15	secondary/ flavonoids
(*R*)-Linalyl beta-vicianoside	$C_{21}H_{36}O_{10}$	$[M + NH_4]^+$	466.265	0	0.798	6.537	secondary/ terpenoids
4-[(*E*)-3-[(2*R*,3*R*,4*S*,5*S*,6*R*)-3-[(2*S*,3*R*,4*R*)-3,4-Dihydroxy-4-(hydroxymethyl)oxolan-2-yl]oxy-4,5-dihydroxy-6-(hydroxymethyl)oxan-2-yl]oxybut-1-enyl]-3,5,5-trimethylcyclohex-2-en-1-one	$C_{22}H_{32}O_{10}$	$[M + H]^+$	457.206	0.003	0.824	6.027	secondary/ terpenoids
Canrenone	$C_{13}H_{32}N_3O_4S$	$[M - H]^-$	325.185	0.021	0.893	12.377	secondary/ terpenoids
Furostan	$C_{46}H_{81}N_7O_{20}$	$[M - H_2O + H]^+$	1034.56	0.007	0.925	6.281	secondary/ terpenoids
Harpagide	$C_{15}H_{24}O_{10}$	$[M + H]^+$	365.105	0.035	0.831	0.627	secondary/ terpenoids

The indicated stereochemistry for the compounds, as well as the positions of the functional groups and the specific isomerism, is based on the greater occurrence of these compounds in nature, in studies with structural characterizations and access to databases. However, this does not exclude the existence of other isomers, especially considering that high-resolution techniques still face limitations in differentiating chiral centers in complex samples such as plant extracts and microorganisms.

L01AT treatment activated secondary metabolic pathways linked to the biosynthesis of phenylpropanoids, flavonoids, and anthocyanins, which is consistent with a stress preparation strategy that does not compromise growth. In contrast, the L01IN treatment predominantly modulated primary metabolic pathways, including lysine biosynthesis and porphyrin metabolism, reflecting metabolic adjustments associated with nitrogen

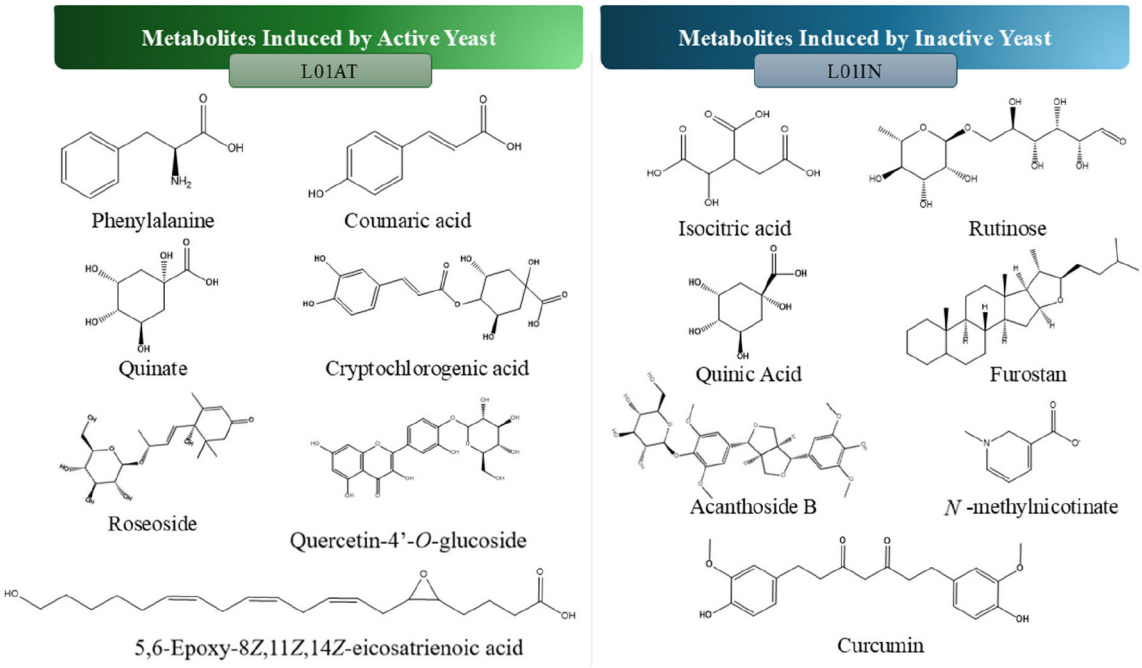

Figure 9. Differentially induced metabolites by inoculation of active yeast (L01AT) and inactivated yeast (L01IN) in tomato seedlings. The metabolites depicted represent those exclusively detected in each treatment, selected as the most biologically relevant compounds associated with plant growth promotion.

assimilation, energy balance, and biomass accumulation. These metabolic distinctions explain the superior growth-promoting performance in seedlings treated with L01IN and demonstrate that yeast-derived compounds, regardless of microbial viability, can function as growth inducers. A total of 73 metabolites were annotated, being 36 and 37 metabolites in tomato seedling leaves inoculated with L01AT and L01IN, respectively.

Although inactivated yeast showed consistent growth-promoting and metabolic effects under the evaluated conditions, its practical advantages related to formulation stability, shelf life, and transport efficiency should be investigated. It is important to emphasize that the metabolic changes observed here should not be interpreted as artifacts of the absence of competitors, but rather as the intrinsic ability of yeast to act as a biochemical elicitor. The induction of secondary metabolism reflects the perception by the plant of yeast-associated molecular patterns and signaling molecules, which are known to operate independently of soil microbial complexity.

Validated in tomato seedlings, the results presented here provide a robust biochemical basis to support the extension of these analyses to other plant organs, cultivated species, and agricultural environments. In this context, the identified metabolic pathways offer a solid foundation for the rational planning of future field trials, reinforcing the potential of yeast-based bioinputs as flexible and chemically sound tools for sustainable agriculture.

Supplementary Information

Supplementary data are available free of charge at http://jbcs.sbq.org.br as PDF file.

Data Availability Statement

The datasets generated and analyzed during the current study are not publicly available due to confidentiality and industrial secrecy constraints, as they contain proprietary information related to formulation processes and experimental conditions. However, the data may be made available from the corresponding author upon reasonable request, subject to evaluation and compliance with confidentiality agreements and applicable institutional or legal restrictions.

Acknowledgments

The authors thank EMBRAPA, UFG, CAPES, and CNPq/MCTI/CT-BIOTEC (440485/2022-3) for support.

Author Contributions

M. A. S.: conceptualization, data curation, formal analysis, investigation, methodology, software, validation, visualization, writing (review and editing); J. C. R. N. and E. A. B.: data curation, formal analysis, investigation, methodology, software, validation, visualization, writing (review and editing); C. A. B. and T. D. M.: methodology, supervision, validation; J. R. M. A.: conceptualization, supervision, writing (review and editing), funding acquisition;

S. B. G.: supervision, funding acquisition, project administration; F. G. S: conceptualization, project administration, supervision, writing (review and editing), funding acquisition; P. V. A.: conceptualization, data curation, formal analysis, investigation, methodology, software, validation, visualization, writing (review and editing), supervision. All authors reviewed the manuscript.

References

1. Punniyakotti, P.; Vinayagam, S.; Rajamohan, R.; Priya, S. D.; Moovendhan, M.; Sundaram, T.; *J. Environ. Chem. Eng.* **2024**, *12*, 113349. [Crossref]
2. Anaduaka, E. G.; Uchendu, N. O.; Asomadu, R. O.; Ezugwu, A. L.; Okeke, E. S.; Ezeorba, T. P. C.; *Heliyon* **2023**, *9*, e15173. [Crossref]
3. Rocha, T. M.; Marcelino, P. R. F.; da Costa, R. A. M.; Rubio-Ribeaux, D.; Barbosa, F. G.; da Silva, S. S.; *Sustainability* **2024**, *16*, 1076. [Crossref]
4. Souza, M. A.; Teixeira, T. S.; Rodrigues-Neto, J. C.; Silva, C. O. G.; Bomfim, C. A.; Barbosa, E. A.; de Siqueira, F. G.; Abdelnur, P. V.; *J. Braz. Chem. Soc.* **2025**, *36*, e-20250163. [Crossref]
5. Kumari, M.; Swarupa, P.; Kesari, K. K.; Kumar, A.; *Life* **2022**, *13*, 12. [Crossref]
6. Leão, E.; *Bioinputs in Brazil - Industry Marker Data*; CropLife Brazil Research, 2025. [Link] accessed in February 2026
7. Ministry of Agriculture, Livestock and Supply; *BIOINPUTS - Increasing Brazilian Biodiversity*, 2022. [Link] accessed in February 2026
8. Nimsi, K. A.; Manjusha, K.; Kathiresan, K.; Arya, H.; *J. Appl. Microbiol.* **2023**, *134*, lxac088. [Crossref]
9. Fu, S. F.; Sun, P. F.; Lu, H. Y.; Wei, J. Y.; Xiao, H. S.; Fang, W. T.; Cheng, B. Y.; Chou, J. Y.; *Fungal Biol.* **2016**, *120*, 433. [Crossref]
10. Fernandez-San Millan, A.; Farran, I.; Larraya, L.; Ancin, M.; Arregui, L. M.; Veramendi, J.; *Microbiol. Res.* **2020**, *237*, 126480. [Crossref]
11. Ruspi, C.; Pierantoni, D. C.; Conti, A.; Scarponi, R.; Corte, L.; Cardinali, G.; *Biol. Fertil. Soils* **2025**, *61*, 293. [Crossref]
12. Amprayn, K.; Rose, M. T.; Kecskés, M.; Pereg, L.; Nguyen, H. T.; Kennedy, I. R.; *Appl. Soil Ecol.* **2012**, *61*, 295. [Crossref]
13. Hernández-Fernández, M.; Cordero-Bueso, G.; Ruiz-Muñoz, M.; Cantoral, J. M.; *Plants* **2021**, *10*, 822. [Crossref]
14. Villas-Bôas, S. G.; Mas, S.; Åkesson, M.; Smedsgaard, J.; Nielsen, J.; *Mass Spectrom. Rev.* **2005**, *24*, 613. [Crossref]
15. Christ, B.; Pluskal, T.; Aubry, S.; Weng, J. K.; *Trends Plant Sci.* **2018**, *23*, 1047. [Crossref]
16. Abdelnur, P. V.; Caldana, C.; Martins, M. C. M.; *Chem. Biol. Technol. Agric.* **2014**, *1*, 22. [Crossref]
17. Kot, A. M.; Kieliszek, M.; Piwowarek, K.; Błażejak, S.; Mussagy, C. U.; *Fungal Biol. Rev.* **2021**, *37*, 41. [Crossref]
18. Dickson, A.; Leaf, A. L.; Hosner, J. F.; *For. Chron.* **1960**, *36*, 10. [Crossref]
19. Yang, H.; Liu, J.; Ma, M.; Tan, Z.; Zhang, K.; Sun, R.; Zhan, X.; Cui, D.; *Plant Stress* **2025**, *16*, 100843. [Crossref]
20. Shah, J.; Zeier, J.; *Front. Plant Sci.* **2013**, *4*, 30. [Crossref]
21. Singh, D. P.; Maurya, S.; Satnami, L.; Renu; Prabha, R.; Sarma, B. K.; Rai, N.; *Plant Stress* **2024**, *14*, 100661. [Crossref]
22. Shabala, S.; White, R. G.; Djordjevic, M. A.; Ruan, Y. L.; *Funct. Plant Biol.* **2015**, *43*, 87. [Crossref]
23. Zhang, H.; Wang, L.; Jin, X.; Bian, L.; Ge, Y.; *Crop J.* **2023**, *11*, 1303. [Crossref]
24. Martínez-Arias, C.; Witzell, J.; Solla, A.; Martin, J. A.; Rodríguez-Calcerrada, J.; *Plant, Cell Environ.* **2022**, *45*, 2875. [Crossref]
25. Rodrigues Neto, J. C.; Vieira, L. R.; Ribeiro, J. A. A.; de Sousa, C. A. F.; Souza Jr., M. T.; Abdelnur, P. V.; *Sci. Rep.* **2021**, *11*, 18271. [Crossref]
26. de Souza, L. P.; Alseekh, S.; Naake, T.; Fernie, A.; *Curr. Protoc. Plant Biol.* **2019**, *4*, e20100. [Crossref]
27. Katajamaa, M.; Miettinen, J.; Orešič, M.; *Bioinformatics* **2006**, *22*, 634. [Crossref]
28. Pluskal, T.; Castillo, S.; Villar-Briones, A.; Orešič, M.; *Bioinformatics* **2010**, *11*, 395. [Crossref]
29. Cuthbertson, D. J.; Johnson, S. R.; Piljac-Žegarac, J.; Kappel, J.; Schäfer, S.; Wüst, M.; Ketchum, R. E. B.; Croteau, R. B.; Marques, J. V.; Davin, L. B.; Lewis, N. G.; Rolf, M.; Kutchan, T. M.; Soejarto, D. D.; Lange, B. M.; *Phytochemistry* **2013**, *91*, 187. [Crossref]
30. Paul, A.; Harrington, P. B.; *TrAC, Trends Anal. Chem.* **2021**, *135*, 116165. [Crossref]
31. Buvé, C.; Saeys, W.; Rasmussen, M.; Neckebroeck, B.; Hendrickx, M.; Grauwet, T.; Van Loey, A.; *Food Res. Int.* **2022**, *151*, 110878. [Crossref]
32. García-Pérez, P.; Becchi, P. P.; Zhang, L.; Rocchetti, G.; Lucini, L.; *Trends Food Sci. Technol.* **2024**, *147*, 104481. [Crossref]
33. Aminu, M.; Ahmad, N. A.; *ACS Omega* **2020**, *5*, 26601. [Crossref]
34. Ruiz-Perez, D.; Guan, H.; Madhivanan, P.; Mathee, K.; Narasimhan, G.; *BMC Bioinf.* **2020**, *21*, 2. [Crossref]
35. Lumumba, V.; Kiprotich, D.; Mpaine, M.; Makena, N.; Kavita, M.; *Am. J. Theor. Appl. Stat.* **2024**, *13*, 127. [Crossref]
36. Clark, R. D.; *J. Comput.- Aided Mol. Des.* **2003**, *17*, 265. [Crossref]
37. Hastie, T.; Tibshirani, R.; Friedman, J.; *The Elements of Statistical Learning*; Springer: New York, NY, USA, 2009. [Crossref]
38. Berrar, D.; *Encycl. Bioinf. Comput. Biol.* **2019**, *1*, 542. [Crossref]
39. Li, S.; Park, Y.; Duraisingham, S.; Strobel, F. H.; Khan, N.; Soltow, Q. A.; Jones, D. P.; Pulendran, B.; *PLoS Comput. Biol.* **2013**, *9* [Crossref]; Global Natural Product Social (GNPS2). [Link] accessed in February 2026

40. Bekatorou, A.; Psarianos, C.; Koutinas, A. A.; *Food Technol. Biotechnol.* **2006**, *44*, 407. [Crossref]
41. Jansa, J.; Šmilauer, P.; Borovička, J.; Hršelová, H.; Forczek, S. T.; Slámová, K.; Řezanka, T.; Rozmoš, M.; Bukovská, P.; Gryndler, M.; *Mycorrhiza* **2020**, *30*, 63. [Crossref]
42. Vargas, M. F.; Mestre, M. V.; Vergara, C.; Maturano, P.; Petrignani, D.; Pesce, V.; Vazquez, F.; *Front. Ind. Microbiol.* **2024**, *2*, 1360263. [Crossref]
43. Conrath, U.; Beckers, G. J. M.; Flors, V.; García-Agustín, P.; Jakab, G.; Mauch, F.; Newman, M. A.; Pieterse, C. M. J.; Poinssot, B.; Pozo, M. J.; Pugin, A.; Schaffrath, U.; Ton, J.; Wendehenne, D.; Zimmerli, L.; Mauch-Mani, B.; *Mol. Plant-Microbe Interact.* **2006**, *19*, 1062. [Crossref]
44. Yu, Y.; Gui, Y.; Li, Z.; Jiang, C.; Guo, J.; Niu, D.; *Plants* **2022**, *11*, 386. [Crossref]
45. Wang, C.; Kuzyakov, Y.; *ISME J.* **2024**, *18*, wrae073. [Crossref]
46. Fraser, C. M.; Chapple, C.; *Arabidopsis Book* **2011**, *9*, e0152. [Crossref]
47. Vogt, T.; *Mol. Plant* **2010**, *3*, 2. [Crossref]
48. Dixon, R. A.; *Nature* **2001**, *411*, 843. [Crossref]
49. Casati, P.; Walbot, V.; *Plant, Cell Environ.* **2005**, *28*, 788. [Crossref]
50. Mierziak, J.; Kostyn, K.; Kulma, A.; *Molecules* **2014**, *19*, 16240. [Crossref]
51. Roy, A.; Khan, A.; Ahmad, I.; Alghamdi, S.; Rajab, B. S.; Babalghith, A. O.; Alshahrani, M. Y.; Islam, S.; Islam, Md. R.; *BioMed Res. Int.* **2022**, *2022*, 445291. [Crossref]
52. Mao, Y.; Luo, J.; Cai, Z.; *Plants* **2025**, *14*, 1847. [Crossref]
53. Liu, J.; Zhou, H.; Song, L.; Yang, Z.; Qiu, M.; Wang, J.; Shi, S.; *Molecules* **2021**, *26*, 3807. [Crossref]
54. Schreiber, L.; *Trends Plant Sci.* **2010**, *15*, 546. [Crossref]
55. Philippe, G.; Sørensen, I.; Jiao, C.; Sun, X.; Fei, Z.; Domozych, D. S.; Rose, J. K.; *Curr. Opin. Plant Biol.* **2020**, *55*, 11. [Crossref]
56. Tzin, V.; Galili, G.; *Arabidopsis Book* **2010**, *8*, e0132. [Crossref]
57. Maeda, H.; Dudareva, N.; *Annu. Rev. Plant Biol.* **2012**, *63*, 73. [Crossref]
58. Parthasarathy, A.; Cross, P. J.; Dobson, R. C. J.; Adams, L. E.; Savka, M. A.; Hudson, A. O.; *Front. Mol. Biosci.* **2018**, *5*, 29. [Crossref]
59. Jaiswal, R.; Sovdat, T.; Vivan, F.; Kuhnert, N.; *J. Agric. Food Chem.* **2010**, *58*, 5471. [Crossref]
60. Widhalm, J. R.; Dudareva, N.; *Mol. Plant* **2015**, *8*, 83. [Crossref]
61. Magaña, A. A.; Kamimura, N.; Soumyanath, A.; Stevens, J. F.; Maier, C. S.; *Plant J.* **2021**, *107*, 1299. [Crossref]
62. Meng, H.; Li, Y.; Lu, B.; Zhang, W.; Shi, X.; Fu, H.; Long, G.; *Agronomy* **2024**, *14*, 1063. [Crossref]
63. Naranjo, L.; de Valmaseda, E. M.; Bañuelos, O.; Lopez, P.; Riaño, J.; Casqueiro, J.; Martin, J. F.; *J. Bacteriol.* **2001**, *183*, 7165. [Crossref]
64. Gatto, G. J.; Boyne, M. T.; Kelleher, N. L.; Walsh, C. T.; *J. Am. Chem. Soc.* **2006**, *128*, 3838. [Crossref]
65. Tahoun, M.; Gee, C. T.; McCoy, V. E.; Sander, P. M.; Müller, C. E.; *RSC Adv.* **2021**, *11*, 7552. [Crossref]
66. Patil, J. R.; Mhatre, K. J.; Yadav, K.; Yadav, L. S.; Srivastava, S.; Nikalje, G. C.; *Discov. Plants* **2024**, *1*, 68. [Crossref]

Submitted: November 11, 2025
Final version online: March 6, 2026